

DYNAMIC CHARACTERISTICS OF PILE GROUPS IN FLUID-FILLED POROELASTIC LAYERS

Shin-ichiro TAKANO¹ And Yuzuru YASUI²

SUMMARY

An analytical method is proposed for dynamic interaction between pile groups and water-saturated soil layers, which are modeled as fluid-filled poroelastic medium. As a fundamental element of this method, three dimensional solutions for the displacements and the pore water pressure in layered fluid-filled poroelastic soil are derived by use of Thin Layer Method when the dynamic point, disc and ring loads or pore water sources are applied. Numerical results of the pore water pressure distributions around the piles are presented and the characteristics are discussed.

INTRODUCTION

When a structure supported by pile groups is built on soft soil in coastal region with relatively high groundwater level, in order to evaluate the earthquake safety of the structure, it is necessary to estimate the response of the soil-pile-structure system properly evaluating the effects of dynamic soil-pile-structure interaction by taking the influence of groundwater into consideration.

In general, motion of the soil containing groundwater can be expressed by a mathematical model of a composite material, which comprises the skeleton composed by soil particles and the pore water to fill the gaps of the particles, i.e. it can be expressed by equations of motion of fluid-filled poroelastic soil. In this paper, we propose an analytical method to practically estimate the effects of dynamic soil-pile-structure interaction using these equations of motion, and we attempt to elucidate the influence of groundwater exerted on the effect of dynamic interaction by evaluating the results of numerical analysis based on the above method.

In dynamic substructure method, which is the basic concept of this paper, the earthquake response of the soil-pile-structure system is divided into two response components, i.e. a response caused only by inertia forces of the structure and the foundation (i.e. dynamic interaction), and a response of a system where masses of the structure and the foundation are neglected (i.e. kinematic interaction). In order to calculate these responses, it is basically important to properly evaluate the soil stiffness around the pile, i.e. the relationship between displacements and loads.

To estimate the soil stiffness, Thin Layer Method is used in this study. The Thin Layer Method is a technique to divide the soil into thin layers, to perform discretization by assuming that each thin layer has uniform and homogeneous physical properties, and to express the relationship between displacements and loads of the horizontally layered soil by means of matrix equation. In the Thin Layer Method, soil has been generally formulated as an elastic medium in the past (Kausel and Peek (1982)). In this paper, however, this concept is extended to the fluid-filled poroelastic soil to newly derive 3-dimensional Green functions, i.e. to calculate soil displacements and pore water pressure when dynamic loads or inflow of pore water is applied to soil. Further, stiffness matrices for soil is constructed using these Green functions and numerical analysis is performed in

¹ Technical Research Institute, Obayashi Corporation, Tokyo, Japan Email: takano@tri.obayashi.co.jp

² Department of Architectural Engineering, Science University of Tokyo, Japan Email: iguchi@rs.noda.sut.ac.jp

accordance with the formulation of the dynamic substructure method. As a result, the characteristics of pore water pressure generated by dynamic and kinematic interactions are elucidated.

GREEN FUNCTIONS FOR LAYERED FLUID-FILLED POROELASTIC SOIL

We consider the fluid-filled poroelastic layers on underlying elastic half-space as shown in Fig.1. Following the formulation of Kausel and Peek (1982) for elastic soil, we define the stress and displacement vectors of this system as follows.

$$\mathbf{U}=(p \ w \ u \ v)^T \quad \mathbf{S}=(\Psi \ \sigma_z \ \tau_{rz} \ \tau_{\theta z}) \quad (1)$$

Here, w , u , v and p denote the displacements in cylindrical co-ordinates z , r , θ and pore water pressure, σ and τ denote the normal and tangential stress components. The variable $\Psi = n(W_f - w)$ is the pore water source flowing through unit area in horizontal plane, where W_f and n are the pore water displacement in z -direction and porosity. These vectors in spatial domain are transformed into those in wave-number domain by the following transformation.

$$\mathbf{U} = \sum_{\mu=1}^{\infty} \mathbf{T}_{\mu} \int_0^{\infty} k \mathbf{C}_{\mu} \bar{\mathbf{U}}_{\mu} dk \quad \bar{\mathbf{U}}_{\mu} = a_{\mu} \int_0^{\infty} r \mathbf{C}_{\mu} \int_0^{2\pi} \mathbf{T}_{\mu} \mathbf{U} d\theta dk \quad (2)$$

Here the bar denotes wave-number domain. Similar expressions are given for \mathbf{S} and $\bar{\mathbf{S}}$. In these expressions, the diagonal matrix \mathbf{T}_{μ} is given by the following expression if the displacements are symmetric with respect to the x -axis.

$$\mathbf{T}_{\mu} = \text{diag}(\cos \mu \theta \ \cos \mu \theta \ \cos \mu \theta \ -\sin \mu \theta) \quad (3)$$

For the anti-symmetric case, $\cos \mu \theta$ and $-\sin \mu \theta$ should be replaced by $\sin \mu \theta$ and $\cos \mu \theta$, respectively. Also, \mathbf{C}_{μ} is given by the following expression.

$$\mathbf{C}_{\mu} = \begin{bmatrix} J_{\mu}(kr) & & & \\ & J_{\mu}(kr) & & \\ & & J'_{\mu}(kr) & \frac{\mu}{kr} J_{\mu}(kr) \\ & & \frac{\mu}{kr} J_{\mu}(kr) & J'_{\mu}(kr) \end{bmatrix} \quad (4)$$

Here $J_{\mu}(kr)$ is a Bessel function of the first kind and μ -th order.

Dynamic equilibrium equations of fluid-filled poroelastic thin layer (for example j -th layer in Fig.1) are converted into those of wave-number domain through transformation (2), and discretized in the vertical direction into the following matrix equations (Rayleigh and Love mode equation) by Galerkin method.

$$\left[k^2 \mathbf{A}_j^R + k \mathbf{B}_j^R + \mathbf{C}_j^R \right] \begin{Bmatrix} \bar{\mathbf{U}}_{j-1}^R \\ \bar{\mathbf{U}}_j^R \end{Bmatrix} = \begin{Bmatrix} \bar{\mathbf{S}}_{j-1}^R \\ \bar{\mathbf{S}}_j^R \end{Bmatrix} \quad \left[k^2 \mathbf{A}_j^L + \mathbf{C}_j^L \right] \begin{Bmatrix} \bar{\mathbf{U}}_{j-1}^L \\ \bar{\mathbf{U}}_j^L \end{Bmatrix} = \begin{Bmatrix} \bar{\mathbf{S}}_{j-1}^L \\ \bar{\mathbf{S}}_j^L \end{Bmatrix} \quad (5)$$

Where the matrices \mathbf{A}_j^R , \mathbf{B}_j^R and \mathbf{C}_j^R , which compose Rayleigh mode, and the matrices \mathbf{A}_j^L and \mathbf{C}_j^L , which compose Love mode, are shown in Table1. And the elements of following vectors are values of layer interface.

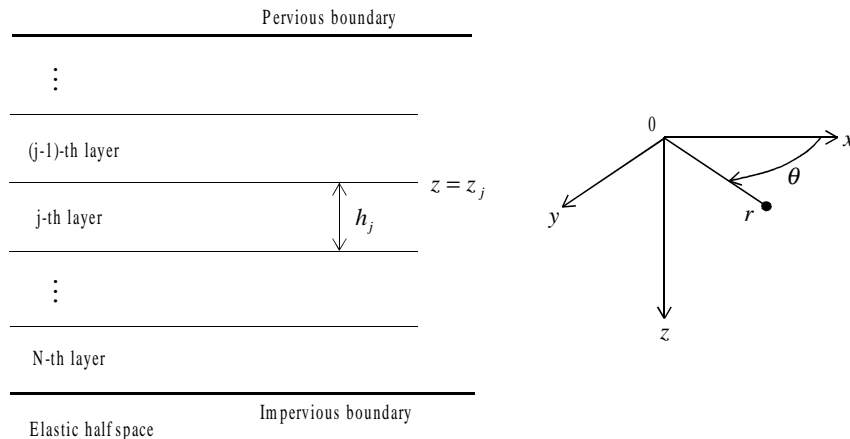


Figure 1: Coordinate system for fluid-filled poroelastic layers

$$\bar{\mathbf{U}}_j^R = \bar{\mathbf{U}}_\mu^R \Big|_{z=z_j} = \left\{ \begin{array}{l} \bar{p} \\ \bar{w} \\ \bar{u} \end{array} \right\}_{z=z_j} \quad \bar{\mathbf{S}}_j^R = \bar{\mathbf{S}}_\mu^R \Big|_{z=z_j} = \left\{ \begin{array}{l} \bar{\Psi} \\ \bar{\sigma}_z \\ \bar{\tau}_{rz} \end{array} \right\}_{z=z_j} \quad \bar{\mathbf{U}}_j^L = \bar{\mathbf{U}}_\mu^L \Big|_{z=z_j} = \{ \bar{v} \}_{z=z_j} \quad \bar{\mathbf{S}}_j^L = \bar{\mathbf{S}}_\mu^L \Big|_{z=z_j} = \{ \bar{\tau}_{\theta z} \}_{z=z_j} \quad (6)$$

Assembling the matrices of each layer, the global matrix equation, which creates the eigenvalue problem for given unit load or pore water source conditions in wave-number domain, is constructed and solved. The solutions are converted into that of spatial domain by transformation (2). The results are as follows.

$$u_m = u(r, \theta, z_m) = a \left(\sum_{l=1}^{3N+2} \phi_u^{ml} \gamma_R^{nl} \frac{d}{dr} f_l + \sum_{l=1}^{N+1} \phi_v^{ml} \gamma_L^{nl} \frac{1}{r} f_l^L \right) \begin{bmatrix} \cos \mu \theta \\ \sin \mu \theta \end{bmatrix} \quad (7)$$

$$v_m = v(r, \theta, z_m) = a \left(\sum_{l=1}^{3N+2} \phi_u^{ml} \gamma_R^{nl} \frac{1}{r} f_l + \sum_{l=1}^{N+1} \phi_v^{ml} \gamma_L^{nl} \frac{d}{dr} f_l^L \right) \begin{bmatrix} -\sin \mu \theta \\ \cos \mu \theta \end{bmatrix} \quad (8)$$

$$w_m = w(r, \theta, z_m) = a \left(\sum_{l=1}^{3N+2} \phi_w^{ml} \gamma_R^{nl} f_l k_l \right) \begin{bmatrix} \cos \mu \theta \\ \sin \mu \theta \end{bmatrix} \quad (9)$$

$$p_m = p(r, \theta, z_m) = a \left(\sum_{l=1}^{3N+2} \phi_p^{ml} \gamma_R^{nl} f_l k_l \right) \begin{bmatrix} \cos \mu \theta \\ \sin \mu \theta \end{bmatrix} \quad (10)$$

Table 1: Elements of matrix equations

$\mathbf{A}^R = \frac{h}{6} \begin{bmatrix} -\frac{2}{F}n^2 & 0 & 0 & -\frac{1}{F}n^2 & 0 & 0 \\ & 2G & 0 & 0 & G & 0 \\ & & 2(\lambda+2G) & 0 & 0 & (\lambda+2G) \\ & & & -\frac{2}{F}n^2 & 0 & 0 \\ \text{symm.} & & & & 2G & 0 \\ & & & & & 2(\lambda+2G) \end{bmatrix}$	$\mathbf{B}^R = \frac{1}{6} \begin{bmatrix} 0 & 0 & 2Tn & 0 & 0 & Tn \\ & 0 & 3(\lambda-G) & 0 & 0 & 3(\lambda+G) \\ & & 0 & Tn & -3(\lambda+G) & 0 \\ & & & 0 & 0 & 2Tn \\ \text{symm.} & & & & 0 & -3(\lambda-G) \\ & & & & & 0 \end{bmatrix}$		
$\mathbf{C}^R = \begin{bmatrix} -\frac{1}{R} \frac{h}{3} n^2 & \frac{2R+N}{2R} n & 0 & -\frac{1}{R} \frac{h}{6} n^2 & -\frac{N}{2R} n & 0 \\ & \frac{\lambda+2G}{h} & 0 & \frac{N}{2R} n & -\frac{\lambda+2G}{h} & 0 \\ & & \frac{G}{h} & 0 & 0 & -\frac{G}{h} \\ \text{symm.} & & & -\frac{1}{R} \frac{h}{3} n^2 & -\frac{2R+N}{2R} n & 0 \\ & & & & \frac{\lambda+2G}{h} & 0 \\ & & & & & \frac{G}{h} \end{bmatrix} + \begin{bmatrix} -\frac{1}{F} \frac{1}{h} n^2 & -\frac{i\omega b}{2F} n & 0 & \frac{1}{F} \frac{1}{h} n^2 & -\frac{i\omega b}{2F} n & 0 \\ & \frac{h}{3} M & 0 & \frac{i\omega b}{2F} n & \frac{h}{6} M & 0 \\ & & \frac{h}{3} M & 0 & 0 & \frac{h}{6} M \\ \text{symm.} & & & -\frac{1}{F} \frac{1}{h} n^2 & \frac{i\omega b}{2F} n & 0 \\ & & & & \frac{h}{3} M & 0 \\ & & & & & \frac{h}{3} M \end{bmatrix}$	$\mathbf{C}^L = \begin{bmatrix} \frac{G}{h} & -\frac{G}{h} \\ -\frac{G}{h} & \frac{G}{h} \end{bmatrix} + \begin{bmatrix} \frac{h}{3} M & \frac{h}{6} M \\ \frac{h}{6} M & \frac{h}{3} M \end{bmatrix}$		
Where	$T = \left(\frac{N}{R} + \frac{i\omega b}{F} \right) h$ $F = i\omega b - \omega^2 \rho_{22}$ $M = i\omega b - \rho_{11} \omega^2 + \frac{b^2 \omega^2}{F}$ n : porosity λ, G : Lamé' modulus of soil skeleton β : bulk modulus of pore water ω : circular frequency	$R = n\beta$ $b = \rho_f g n^2 / k$ $\rho_{11} = (1-n)\rho$ ρ : mass density of soil particle ρ_f : mass density of pore water k : permeability h : thickness of thin layer	$N = (1-n)\beta$ g : gravitational acceleration $\rho_{22} = n\rho_f$

Table 2: List of factors

Load or pore water source	a	γ_R^{nl}	γ_L^{nl}	f_l	μ
Horizontal point load	$1/(4i)$	φ_u^{nl}	φ_v^{nl}	$H_1^{(2)}(k_l r)/k_l$	1
Vertical point load	$1/(4i)$	φ_w^{nl}	0	$H_0^{(2)}(k_l r)/k_l$	0
Pore water point source	$1/(4i)$	φ_p^{nl}	0	$H_0^{(2)}(k_l r)/k_l$	0
Horizontal disc load	$1/(\pi R)$	φ_u^{nl}	φ_v^{nl}	I_{3l}	1
Vertical disc load	$1/(\pi R)$	φ_w^{nl}	0	I_{1l}/k_l	0
Pore water disc source	$1/(\pi R)$	φ_p^{nl}	0	I_{1l}/k_l	0
Horizontal ring load	$1/(2\pi)$	φ_u^{nl}	φ_v^{nl}	I_{1l}^*	1
Vertical ring load	$1/(2\pi)$	φ_w^{nl}	0	I_{4l}/k_l	0
Rocking ring load	$1/(\pi R)$	φ_w^{nl}	0	I_{2l}/k_l	1
Pore water uniform ring source	$1/(2\pi)$	φ_p^{nl}	0	I_{4l}/k_l	0
Pore water inclined ring source	$1/(\pi R)$	φ_p^{nl}	0	I_{2l}/k_l	1

Table 3: Representation of integrals

$$\begin{aligned}
I_{1l} &= \int_0^\infty \frac{1}{k^2 - k_l^2} J_0(kr) J_1(kR) dk = \begin{cases} \frac{\pi}{2ik_l} J_0(k_l r) H_1^{(2)}(k_l R) - \frac{1}{Rk_l^2} & (0 \leq r \leq R) \\ \frac{\pi}{2ik_l} J_1(k_l R) H_0^{(2)}(k_l r) & (R \leq r) \end{cases} \\
I_{2l} &= \int_0^\infty \frac{k}{k^2 - k_l^2} J_1(kr) J_1(kR) dk = \begin{cases} \frac{\pi}{2i} J_1(k_l r) H_1^{(2)}(k_l R) & (0 \leq r \leq R) \\ \frac{\pi}{2i} J_1(k_l R) H_1^{(2)}(k_l r) & (R \leq r) \end{cases} \\
I_{3l} &= \int_0^\infty \frac{1}{k(k^2 - k_l^2)} J_1(kr) J_1(kR) dk = \begin{cases} \frac{\pi}{2ik_l^2} J_1(k_l r) H_1^{(2)}(k_l R) - \frac{r}{2Rk_l^2} & (0 \leq r \leq R) \\ \frac{\pi}{2ik_l^2} J_1(k_l R) H_1^{(2)}(k_l r) - \frac{R}{2rk_l^2} & (R \leq r) \end{cases} \\
I_{4l} &= \int_0^\infty \frac{k}{k^2 - k_l^2} J_0(kr) J_0(kR) dk = \begin{cases} \frac{\pi}{2i} J_0(k_l r) H_0^{(2)}(k_l R) & (0 \leq r \leq R) \\ \frac{\pi}{2i} J_0(k_l R) H_0^{(2)}(k_l r) & (R \leq r) \end{cases}
\end{aligned}$$

Where $k_l (l=1,2,\dots,3N+2)$ and $k_l^L (l=1,2,\dots,N+1)$ are eigenvalues of Rayleigh and Love mode matrix equations, respectively. φ_p^{ml} , φ_w^{ml} , $\varphi_u^{ml} (l=1,2,\dots,3N+2)$ and $\varphi_v^{ml} (l=1,2,\dots,N+1)$ are m-th components of related eigenvectors corresponding to p , w , u and v , respectively. The factors a , γ_R^{nl} , γ_L^{nl} , f_l and μ are listed in Table2 for each load or pore water source boundary conditions, where $H_\mu^{(2)}$ is a Hankel function of the second kind and μ -th order, and the functions I_{1l} , I_{1l}^* , I_{2l} , I_{3l} and I_{4l} are constructed by Bessel and Hankel functions as shown in Table3. When the function f_l has superscript L , the eigenvalue k_l is replaced by k_l^L . The value R in factor a is the radius of disc/ring where loads or pore water sources are applied.

FORMULATION FOR PILE GROUPS

In order to calculate the response of soil-pile-structure system according to the theory of substructure method, it is basically important to properly evaluate the stiffness matrices of soil-pile system, i.e. the relationship between displacements and loads. In this paper, the stiffness matrices of soil-pile system are calculated as follows (fig.2). The stiffness matrices of soil layers are constructed by the solutions of the Thin Layer Method, then those of soil

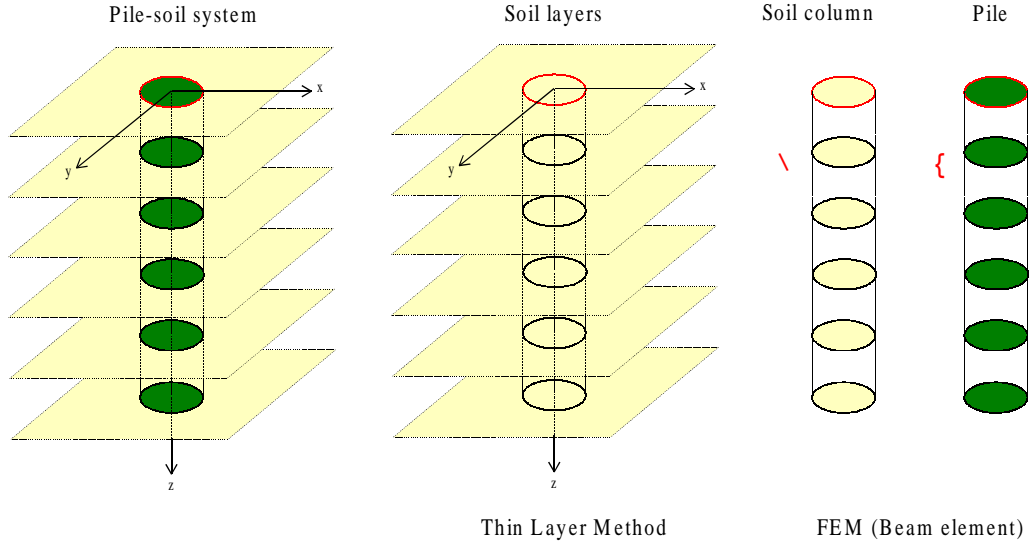


Figure 2: Stiffness matrices of pile-soil system

columns by finite element procedure are subtracted, and those of pile columns derived by the same procedure are added.

The stiffness matrices of soil layers are derived from following relation.

$$\begin{Bmatrix} p_i \\ \Theta_i^{py} \\ \Theta_i^{px} \\ u_i^z \\ u_i^x \\ \Theta_i^y \\ u_i^y \\ \Theta_i^x \end{Bmatrix} = \begin{bmatrix} \alpha_{11} & 0 & 0 & \alpha_{14} & 0 & 0 & 0 & 0 \\ 0 & \alpha_{22} & 0 & 0 & \alpha_{25} & \alpha_{26} & 0 & 0 \\ 0 & 0 & \alpha_{33} & 0 & 0 & 0 & \alpha_{37} & \alpha_{38} \\ \alpha_{41} & 0 & 0 & \alpha_{44} & 0 & 0 & 0 & 0 \\ 0 & \alpha_{52} & 0 & 0 & \alpha_{55} & \alpha_{56} & 0 & 0 \\ 0 & \alpha_{62} & 0 & 0 & \alpha_{65} & \alpha_{66} & 0 & 0 \\ 0 & 0 & \alpha_{73} & 0 & 0 & 0 & \alpha_{77} & \alpha_{78} \\ 0 & 0 & \alpha_{83} & 0 & 0 & 0 & \alpha_{87} & \alpha_{88} \end{bmatrix} \begin{Bmatrix} \Psi_j \\ \Sigma_j^y \\ \Sigma_j^x \\ F_j^z \\ F_j^x \\ M_j^y \\ F_j^y \\ M_j^x \end{Bmatrix} \quad (11)$$

Where the left-hand-side vector consists of pore water pressure and displacements. The elements, p_i , Θ_i^{py} , Θ_i^{px} , u_i^z , u_i^x , Θ_i^y , u_i^y and Θ_i^x , are uniformly distributed pore water pressure, inclined distributed pore water pressure around y-axis, the same one around x-axis, z-directional displacement, x-directional displacement, rotation around y-axis, y-directional displacement and rotation around x-axis, respectively. On the other hand, the right-hand-side vector consists of pore water injection and loads. The elements, Ψ_j , Σ_j^y , Σ_j^x , F_j^z , F_j^x , M_j^y , F_j^y and M_j^x , are uniformly distributed pore water injection, inclined distributed pore water injection around y-axis, the same one around x-axis, z-directional load, x-directional load, moment around y-axis, y-directional load and moment around x-axis, respectively (Fig.3). Each element can be calculated as follows according to the solutions in the previous section when loads or pore water sources are applied at j-th layer.

$$u_i^x = u^x(r, \theta, z_i) = u(r, \theta, z_i) \cos \theta - v(r, \theta, z_i) \sin \theta \quad (12)$$

$$u_i^y = u^y(r, \theta, z_i) = u(r, \theta, z_i) \sin \theta + v(r, \theta, z_i) \cos \theta \quad (13)$$

$$u_i^z = u^z(r, \theta, z_i) = w(r, \theta, z_i) \quad (14)$$

$$p_i = p(r, \theta, z_i)$$

$$\Theta_i^y = -\frac{1}{2R} (w(R, 0, z_i) - w(R, \pi, z_i)) \quad (15)$$

$$\Theta_i^x = \frac{1}{2R} \left(w\left(R, \frac{\pi}{2}, z_i\right) - w\left(R, \frac{3\pi}{2}, z_i\right) \right) \quad (16)$$

$$\Theta_i^{py} = -\frac{1}{2R} (p(R, 0, z_i) - p(R, \pi, z_i)) \quad (17)$$

$$\Theta_i^{px} = \frac{1}{2R} \left(p\left(R, \frac{\pi}{2}, z_i\right) - p\left(R, \frac{3\pi}{2}, z_i\right) \right) \quad (18)$$

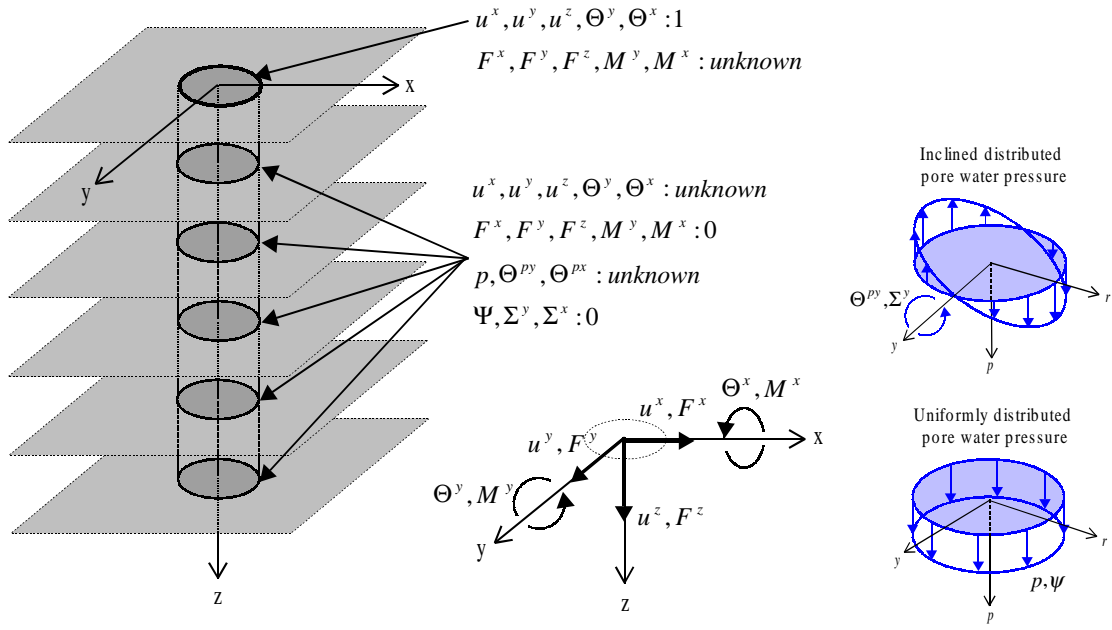


Figure 3: Relation between displacement, pore water pressure and load, pore water injection

The dynamic pile-soil interaction analysis of pile groups in the fluid-filled poroelastic soil is a mixed boundary value problem (Fig.3). At the pile cap, the displacements and the bending angles are given, and the forces and moments are unknown. At the pile nodes except pile cap, the displacements and the bending angles are unknown, and the forces and moments are given, or zero in case there are no external loads. And, at the pile nodes except pile cap, the pore water pressure and the angle of pore water pressure distribution is unknown, and the uniformly and inclined distributed pore water injections are zero.

NUMERICAL RESULTS

Fig.4 shows the model structure, which is a 5-story building constructed on pile groups. The 36 piles are embedded in the surface layer on elastic half-space. There are 2 cases of surface layer type, which are loose sand case and dense sand case, and both of them are filled with pore water (Table4). The soil is subjected to the vertically incident SV wave, such that the observed one at the free surface should be El Centro/NS data, whose maximum velocity is normalized to 10 kine. The calculation is performed in the frequency domain, and transformed to the time domain by FFT.

Fig.5 shows the distribution of the maximum pore water pressure along the piles, which are located near center (No.1), at edge corner (No.9) and outer side (No.3 and No.7 in Fig.4). The required pore water pressure is

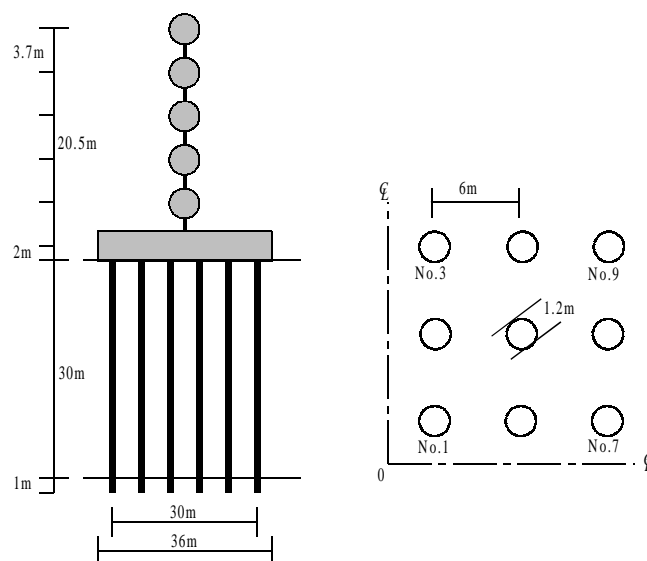


Figure 4: Calculation model

Table 4: Material properties of soil

			loose sand	dense sand
Surface layer 30m	Poroelastic	Mass density of soil particle (tf/m ³)	2.65	2.65
		Shear modulus of soil skeleton (tf/m ²)	0.41x10 ⁴	1.22x10 ⁴
		Poisson's ration of soil skeleton	0.3	0.3
		Porosity	0.454	0.394
		Permeability (m/sec)	1.0x10 ⁻⁴	1.0x10 ⁻⁵
		Bulk modulus of pore water (tf/m ²)	0.4327x10 ⁴	0.3939x10 ⁵
Half space	Elastic	Mass density (tf/m ³)	1.9	
		Shear modulus (tf/m ²)	3.102x10 ⁴	
		Poisson's ration	0.4	

separated into the one uniformly distributed around the pile section and the one inclined distributed around the pile section.

Fig.6 shows the distribution of the maximum pore water pressure along the No.9 pile, which are separated into the dynamic interaction effect and kinematic one. The results are also separated into the uniformly distributed pore water pressure and inclined distributed one. Dynamic interaction effect is stronger in case of uniformly distributed pore water pressure. On the other hand, in case of inclined distributed one, the dynamic interaction effect is stronger than the kinematic one near the pile cap, and the kinematic one is stronger at the end of the pile.

CONCLUSIONS

- Green functions for layered fluid-filled poroelastic soil were derived in accordance with three dimensional Thin Layer Method. As the boundary conditions applied from outside, Point loads, Disk loads, and ring loads, and further, the injected volume of pore water from a source were considered. The boundary conditions where pore water flows in/out the ring were further divided to two conditions, i.e.

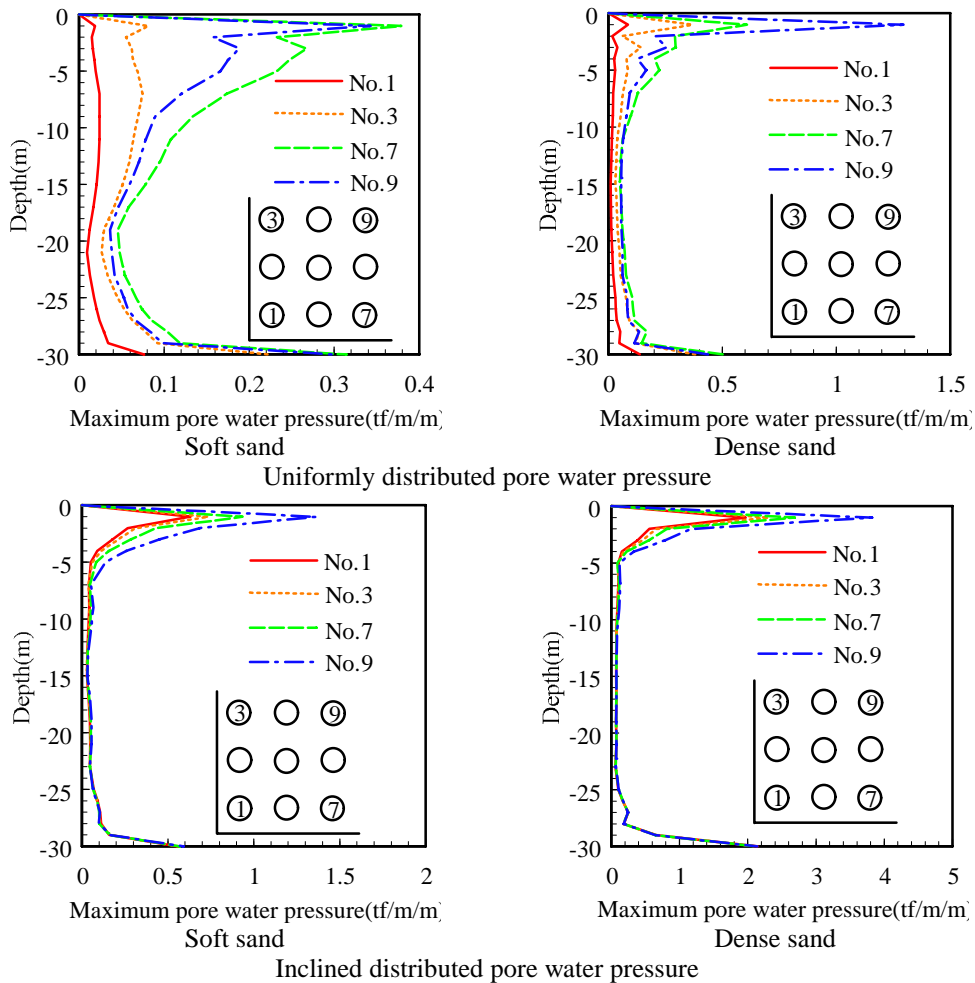


Figure 5: Maximum pore water pressure distribution (difference of location)

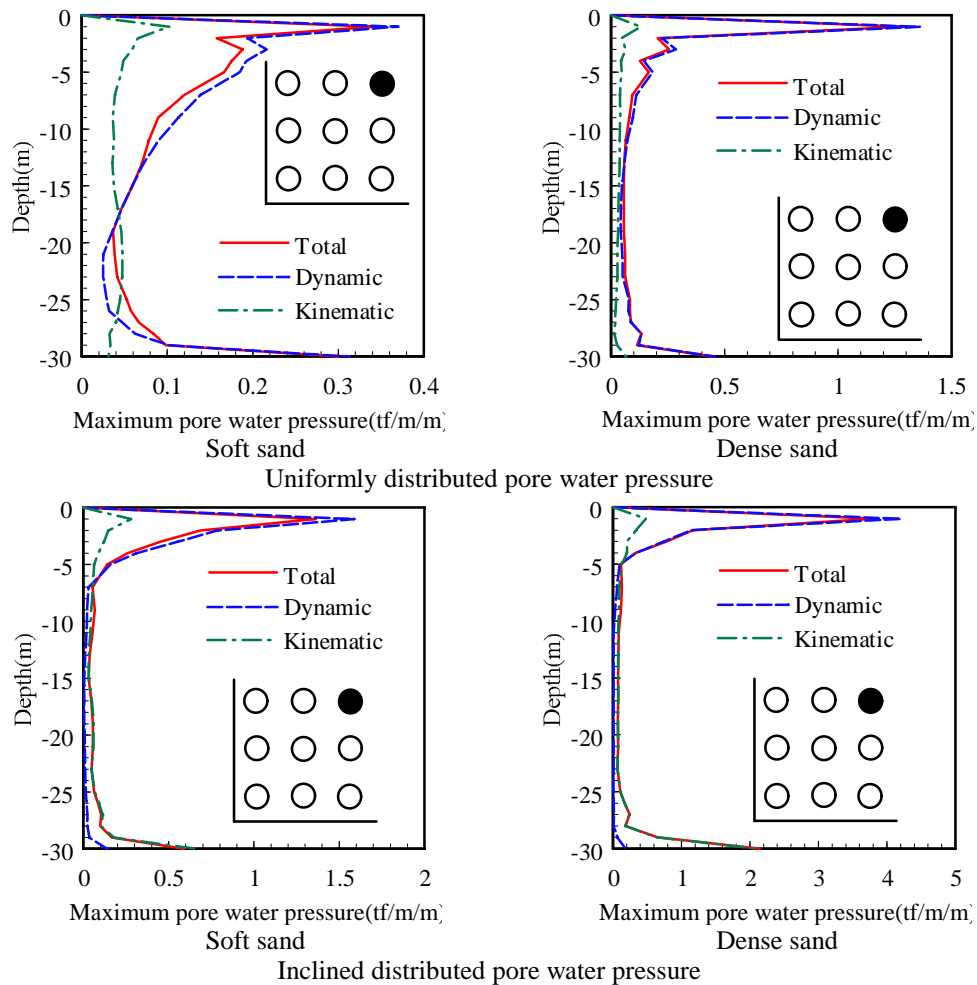


Figure 6: Maximum pore water pressure distribution (dynamic interaction and kinematic interaction)

to the case where it flows in/out with uniform distribution around the pile section or to the case where it flows in/out with inclined distribution.

2. Stiffness matrices for soil were constructed using various Green functions for dynamic loads, and dynamic interaction analysis between pile groups and fluid-filled poroelastic soil was formulated based on the substructure method.
3. The results of calculation of the pore water pressure generated around the piles are shown, and the features of these results were discussed.

REFERENCES

1. Bougacha, S., Tassoulas, J. L. and Roesset, J. M. (1993), "Analysis of foundations on fluid-filled poroelastic stratum", *J. Engrg. Mech.*, ASCE, **119**(8), 1632-1648.
2. Kausel, E. and Peek, R. (1986), "Dynamic loads in the interior of a layered stratum : An explicit solution", *Bull. Seismol. Soc. Am.*, **72**, 1459-1481.
3. Takano, S., Yasui, Y. and Iguchi, M. (1998), "Point load solutions on layered fluid-filled poroelastic soil by thin layered element method and its application", *J. Struct. Constr. Eng.*, AIJ, No.504, 49-56, in Japanese.
4. Takano, S., Yasui, Y. and Iguchi, M. (1998), "Dynamic soil-structure interaction analysis of single piles in layered fluid-filled poroelastic soil by thin layered element method", *J. Struct. Constr. Eng.*, AIJ, No.512, 91-98, in Japanese.
5. Takano, S., Yasui, Y. and Iguchi, M. (1999), "Dynamic soil-structure interaction analysis of pile groups in layered fluid-filled poroelastic soil by thin layered element method", *J. Struct. Constr. Eng.*, AIJ, No.515, 67-74, in Japanese.

Takano, S., Yasui, Y. and Iguchi, M. (1998), "Dynamic load solutions for layered fluid-filled poroelastic soil by thin layer method", *Proceedings of the 12th Engineering Mechanics Conference, ASCE*, 470-473.